

Determination of the number of $\psi(3686)$ events taken at BESIII*

M. Ablikim (麦迪娜)¹ M. N. Achasov^{4,c} P. Adlarson⁷⁵ O. Afedulidis³ X. C. Ai (艾小聪)⁸⁰ R. Aliberti³⁵
 A. Amoroso^{74A,74C} Q. An (安琪)^{71,58,a} Y. Bai (白羽)⁵⁷ O. Bakina³⁶ I. Balossino^{29A} Y. Ban (班勇)^{46,h}
 H.-R. Bao (包浩然)⁶³ V. Batozskaya^{1,44} K. Begzsuren³² N. Berger³⁵ M. Berlowski⁴⁴ M. Bertani^{28A} D. Bettoni^{29A}
 F. Bianchi^{74A,74C} E. Bianco^{74A,74C} A. Bortone^{74A,74C} I. Boyko³⁶ R. A. Briere⁵ A. Brueggemann⁶⁸ H. Cai (蔡浩)⁷⁶
 X. Cai (蔡啸)^{1,58} A. Calcaterra^{28A} G. F. Cao (曹国富)^{1,63} N. Cao (曹宁)^{1,63} S. A. Cetin^{62A} J. F. Chang (常劲帆)^{1,58}
 G. R. Che (车国荣)⁴³ G. Chelkov^{36,b} C. Chen (陈琛)⁴³ C. H. Chen (陈春卉)⁹ Chao Chen (陈超)⁵⁵ G. Chen (陈刚)¹
 H. S. Chen (陈和生)^{1,63} H. Y. Chen (陈弘扬)²⁰ M. L. Chen (陈玛丽)^{1,58,63} S. J. Chen (陈申见)⁴²
 S. L. Chen (陈思璐)⁴⁵ S. M. Chen (陈少敏)⁶¹ T. Chen (陈通)^{1,63} X. R. Chen (陈旭荣)^{31,63} X. T. Chen (陈肖婷)^{1,63}
 Y. B. Chen (陈元柏)^{1,58} Y. Q. Chen³⁴ Z. J. Chen (陈卓俊)^{25,i} Z. Y. Chen (陈正元)^{1,63} S. K. Choi^{10A} G. Cibinetto^{29A}
 F. Cossio^{74C} J. J. Cui (崔佳佳)⁵⁰ H. L. Dai (代洪亮)^{1,58} J. P. Dai (代建平)⁷⁸ A. Dbeyssi¹⁸ R. E. de Boer³
 D. Dedovich³⁶ C. Q. Deng (邓创旗)⁷² Z. Y. Deng (邓子艳)¹ A. Denig³⁵ I. Denysenko³⁶ M. Destefanis^{74A,74C}
 F. De Mori^{74A,74C} B. Ding (丁彪)^{66,1} X. X. Ding (丁晓萱)^{46,h} Y. Ding (丁勇)⁴⁰ Y. Ding (丁逸)³⁴ J. Dong (董静)^{1,58}
 L. Y. Dong (董燎原)^{1,63} M. Y. Dong (董明义)^{1,58,63} X. Dong (董翔)⁷⁶ M. C. Du (杜蒙川)¹ S. X. Du (杜书先)⁸⁰
 Y. Y. Duan (段尧予)⁵⁵ Z. H. Duan (段宗欢)⁴² P. Egorov^{36,b} Y. H. Fan (范宇晗)⁴⁵ J. Fang (方建)^{1,58} J. Fang (方进)⁵⁹
 S. S. Fang (房双世)^{1,63} W. X. Fang (方文兴)¹ Y. Fang (方易)¹ Y. Q. Fang (方亚泉)^{1,58} R. Farinelli^{29A}
 L. Fava^{74B,74C} F. Feldbauer³ G. Felici^{28A} C. Q. Feng (封常青)^{71,58} J. H. Feng (冯俊华)⁵⁹ Y. T. Feng (冯琦潼)^{71,58}
 M. Fritsch³ C. D. Fu (傅成栋)¹ J. L. Fu (傅金林)⁶³ Y. W. Fu (傅亦威)^{1,63} H. Gao (高涵)⁶³ X. B. Gao (高鑫博)⁴¹
 Y. N. Gao (高原宁)^{46,h} Yang Gao (高扬)^{71,58} S. Garbolino^{74C} I. Garzia^{29A,29B} L. Ge (葛玲)⁸⁰ P. T. Ge (葛潘婷)⁷⁶
 Z. W. Ge (葛振武)⁴² C. Geng (耿聪)⁵⁹ E. M. Gersabeck⁶⁷ A. Gilman⁶⁹ K. Goetzen¹³ L. Gong (龚丽)⁴⁰
 W. X. Gong (龚文焯)^{1,58} W. Gradl³⁵ S. Gramigna^{29A,29B} M. Greco^{74A,74C} M. H. Gu (顾旻皓)^{1,58} Y. T. Gu (顾运厅)¹⁵
 C. Y. Guan (关春懿)^{1,63} Z. L. Guan (关志林)²² A. Q. Guo (郭爱强)^{31,63} L. B. Guo (郭立波)⁴¹ M. J. Guo (国梦娇)⁵⁰
 R. P. Guo (郭如盼)⁴⁹ Y. P. Guo (郭玉萍)^{12,g} A. Guskov^{36,b} J. Gutierrez²⁷ K. L. Han (韩坤霖)⁶³ T. T. Han (韩婷婷)¹
 F. Hanisch³ X. Q. Hao (郝喜庆)¹⁹ F. A. Harris⁶⁵ K. K. He (何凯凯)⁵⁵ K. L. He (何康林)^{1,63} F. H. Heinsius³
 C. H. Heinz³⁵ Y. K. Heng (衡月昆)^{1,58,63} C. Herold⁶⁰ T. Holtmann³ P. C. Hong (洪鹏程)³⁴ G. Y. Hou (侯国一)^{1,63}
 X. T. Hou (侯贤涛)⁶³ Y. R. Hou (侯颖锐)⁶³ Z. L. Hou (侯治龙)¹ B. Y. Hu (胡碧颖)⁵⁹ H. M. Hu (胡海明)^{1,63}
 J. F. Hu (胡继峰)^{56,j} S. L. Hu (胡圣亮)^{12,g} T. Hu (胡涛)^{1,58,63} Y. Hu (胡誉)¹ G. S. Huang (黄光顺)^{71,58}
 K. X. Huang (黄凯旋)⁵⁹ L. Q. Huang (黄麟钦)^{31,63} X. T. Huang (黄性涛)⁵⁰ Y. P. Huang (黄燕萍)¹ T. Hussain⁷³
 F. Hölzken³ N. Hüsken³⁵ N. in der Wiesche⁶⁸ J. Jackson²⁷ S. Janchiv³² J. H. Jeong^{10A} Q. Ji (纪全)¹
 Q. P. Ji (姬清平)¹⁹ W. Ji (季旺)^{1,63} X. B. Ji (季晓斌)^{1,63} X. L. Ji (季筱璐)^{1,58} Y. Y. Ji (吉钰瑶)⁵⁰

Received 12 March 2024; Accepted 17 June 2024; Published online 18 June 2024

* The BESIII Collaboration thanks the staff of BEPCII and the IHEP computing center for their strong support. This work is supported in part by National Key R&D Program of China under Contracts Nos. 2020YFA0406300, 2020YFA0406400; National Natural Science Foundation of China (NSFC) under Contracts Nos. 12150004, 11635010, 11735014, 11835012, 11935015, 11935016, 11935018, 11961141012, 12025502, 12035009, 12035013, 12061131003, 12192260, 12192261, 12192262, 12192263, 12192264, 12192265, 12221005, 12225509, 12235017; the Program of Science and Technology Development Plan of Jilin Province of China under Contract Nos. 20210508047RQ and 20230101021JC; the Chinese Academy of Sciences (CAS) Large-Scale Scientific Facility Program; the CAS Center for Excellence in Particle Physics (CCEPP); Joint Large-Scale Scientific Facility Funds of the NSFC and CAS under Contract No. U1832207; CAS Key Research Program of Frontier Sciences under Contracts Nos. QYZDJ-SSW-SLH003, QYZDJ-SSW-SLH040; 100 Talents Program of CAS; The Institute of Nuclear and Particle Physics (INPAC) and Shanghai Key Laboratory for Particle Physics and Cosmology; European Union's Horizon 2020 research and innovation programme under Marie Skłodowska-Curie grant agreement under Contract No. 894790; German Research Foundation DFG under Contracts Nos. 455635585, Collaborative Research Center CRC 1044, FOR5327, GRK 2149; Istituto Nazionale di Fisica Nucleare, Italy; Ministry of Development of Turkey under Contract No. DPT2006K-120470; National Research Foundation of Korea under Contract No. NRF-2022R1A2C1092335; National Science and Technology fund of Mongolia; National Science Research and Innovation Fund (NSRF) via the Program Management Unit for Human Resources & Institutional Development, Research and Innovation of Thailand under Contract No. B16F640076; Polish National Science Centre under Contract No. 2019/35/O/ST2/02907; The Swedish Research Council; U. S. Department of Energy under Contract No. DE-FG02-05ER41374.



Content from this work may be used under the terms of the Creative Commons Attribution 3.0 licence. Any further distribution of this work must maintain attribution to the author(s) and the title of the work, journal citation and DOI. Article funded by SCOAP³ and published under licence by Chinese Physical Society and the Institute of High Energy Physics of the Chinese Academy of Sciences and the Institute of Modern Physics of the Chinese Academy of Sciences and IOP Publishing Ltd

- X. Q. Jia (贾晓倩)⁵⁰ Z. K. Jia (贾泽坤)^{71,58} D. Jiang (姜地)^{1,63} H. B. Jiang (姜候兵)⁷⁶ P. C. Jiang (蒋沛成)^{46,h}
 S. S. Jiang (姜赛俊)³⁹ T. J. Jiang (蒋庭俊)¹⁶ X. S. Jiang (江晓山)^{1,58,63} Y. Jiang (蒋艺)⁶³ J. B. Jiao (焦健斌)⁵⁰
 J. K. Jiao (焦俊坤)³⁴ Z. Jiao (焦铮)²³ S. Jin (金山)⁴² Y. Jin (金毅)⁶⁶ M. Q. Jing (荆茂强)^{1,63} X. M. Jing (景新媚)⁶³
 T. Johansson⁷⁵ S. Kabana³³ N. Kalantar-Nayestanaki⁶⁴ X. L. Kang (康晓琳)⁹ X. S. Kang (康晓坤)⁴⁰
 M. Kavatsyuk⁶⁴ B. C. Ke (柯百谦)⁸⁰ V. Khachatryan²⁷ A. Khoukaz⁶⁸ R. Kiuchi¹ O. B. Kolcu^{62A} B. Kopt³
 M. Kuessner³ X. Kui (奎贤)^{1,63} N. Kumar²⁶ A. Kupsc^{44,75} W. Kühn³⁷ J. J. Lane⁶⁷ P. Larin¹⁸ L. Lavezzi^{74A,74C}
 T. T. Lei (雷天天)^{71,58} Z. H. Lei (雷祚弘)^{71,58} M. Lellmann³⁵ T. Lenz³⁵ C. Li (李聪)⁴³ C. Li (李翠)⁴⁷
 C. H. Li (李春花)³⁹ Cheng Li (李澄)^{71,58} D. M. Li (李德民)⁸⁰ F. Li (李飞)^{1,58} G. Li (李刚)¹ H. B. Li (李海波)^{1,63}
 H. J. Li (李惠静)¹⁹ H. N. Li (李衡讷)^{56j} Hui Li (李慧)⁴³ J. R. Li (李嘉荣)⁶¹ J. S. Li (李静舒)⁵⁹ Ke Li (李科)¹
 L. J. Li (李林健)^{1,63} L. K. Li (李龙科)¹ Lei Li (李蕾)⁴⁸ M. H. Li (李明浩)⁴³ P. R. Li (李培荣)^{38,k,1}
 Q. M. Li (李启铭)^{1,63} Q. X. Li (李起鑫)⁵⁰ R. Li (李燃)^{17,31} S. X. Li (李素娴)¹² T. Li (李腾)⁵⁰ W. D. Li (李卫东)^{1,63}
 W. G. Li (李卫国)^{1,a} X. Li (李旭)^{1,63} X. H. Li (李旭红)^{71,58} X. L. Li (李晓玲)⁵⁰ X. Z. Li (李绪泽)⁵⁹
 Xiaoyu Li (李骁宇)^{1,63} Y. G. Li (李彦谷)^{46,h} Z. J. Li (李志军)⁵⁹ Z. X. Li (李振轩)¹⁵ Z. Y. Li (李紫阳)⁷⁸
 C. Liang (梁畅)⁴² H. Liang (梁浩)^{1,63} H. Liang (梁昊)^{71,58} Y. F. Liang (梁勇飞)⁵⁴ Y. T. Liang (梁羽铁)^{31,63}
 G. R. Liao (廖广睿)¹⁴ L. Z. Liao (廖龙洲)⁵⁰ Y. P. Liao (廖一朴)^{1,63} J. Libby²⁶ A. Limphirat⁶⁰ C. C. Lin (蔺长城)⁵⁵
 D. X. Lin (林德旭)^{31,63} T. Lin (林韬)¹ B. J. Liu (刘北江)¹ B. X. Liu (刘宝鑫)⁷⁶ C. Liu (刘成)³⁴
 C. X. Liu (刘春秀)¹ F. H. Liu (刘福虎)⁵³ Fang Liu (刘芳)¹ Feng Liu (刘峰)⁶ G. M. Liu (刘国明)^{56j}
 H. Liu (刘昊)^{38,k,1} H. B. Liu (刘宏邦)¹⁵ H. M. Liu (刘怀民)^{1,63} Huanhuan Liu (刘欢欢)¹ Huihui Liu (刘汇慧)²¹
 J. B. Liu (刘建北)^{71,58} J. Y. Liu (刘晶译)^{1,63} K. Liu (刘凯)^{38,k,1} K. Y. Liu (刘魁勇)⁴⁰ Ke Liu (刘珂)²²
 L. Liu (刘亮)^{71,58} L. C. Liu (刘良辰)⁴³ Lu Liu (刘露)⁴³ M. H. Liu (刘美宏)^{12,g} P. L. Liu (刘佩莲)¹ Q. Liu (刘倩)⁶³
 S. B. Liu (刘树彬)^{71,58} T. Liu (刘桐)^{12,g} W. K. Liu (刘维克)⁴³ W. M. Liu (刘卫民)^{71,58} X. Liu (刘翔)^{38,k,1}
 X. Liu (刘鑫)³⁹ Y. Liu (刘英)^{38,k,1} Y. Liu (刘义)⁸⁰ Y. B. Liu (刘玉斌)⁴³ Z. A. Liu (刘振安)^{1,58,63} Z. D. Liu (刘宗德)⁹
 Z. Q. Liu (刘智青)⁵⁰ X. C. Lou (娄辛丑)^{1,58,63} F. X. Lu (卢飞翔)⁵⁹ H. J. Lu (吕海江)²³ J. G. Lu (吕军光)^{1,58}
 X. L. Lu (陆小玲)¹ Y. Lu (卢宇)⁷ Y. P. Lu (卢宇鹏)^{1,58} Z. H. Lu (卢泽辉)^{1,63} C. L. Luo (罗成林)⁴¹
 J. R. Luo (罗家瑞)⁵⁹ M. X. Luo (罗民兴)⁷⁹ T. Luo (罗涛)^{12,g} X. L. Luo (罗小兰)^{1,58} X. R. Lyu (吕晓睿)⁶³
 Y. F. Lyu (吕翌丰)⁴³ F. C. Ma (马凤才)⁴⁰ H. Ma (马衡)⁷⁸ H. L. Ma (马海龙)¹ J. L. Ma (马俊力)^{1,63}
 L. L. Ma (马连良)⁵⁰ M. M. Ma (马明明)^{1,63} Q. M. Ma (马秋梅)¹ R. Q. Ma (马润秋)^{1,63} T. Ma (马腾)^{71,58}
 X. T. Ma (马晓天)^{1,63} X. Y. Ma (马骁妍)^{1,58} Y. Ma (马尧)^{46,h} Y. M. Ma (马玉明)³¹ F. E. Maas¹⁸ M. Maggiora^{74A,74C}
 S. Malde⁶⁹ Y. J. Mao (冒亚军)^{46,h} Z. P. Mao (毛泽普)¹ S. Marcello^{74A,74C} Z. X. Meng (孟召霞)⁶⁶
 J. G. Messchendorp^{13,64} G. Mezzadri^{29A} H. Miao (妙哈)^{1,63} T. J. Min (闵天觉)⁴² R. E. Mitchell²⁷
 X. H. Mo (莫晓虎)^{1,58,63} B. Moses²⁷ N. Yu. Muchnoi^{4,c} J. Muskalla³⁵ Y. Nefedov³⁶ F. Nerling^{18,e}
 L. S. Nie (聂麟苏)²⁰ I. B. Nikolaev^{4,c} Z. Ning (宁哲)^{1,58} S. Nisar^{11,m} Q. L. Niu (牛祺乐)^{38,k,1} W. D. Niu (牛文迪)⁵⁵
 Y. Niu (牛艳)⁵⁰ S. L. Olsen⁶³ Q. Ouyang (欧阳群)^{1,58,63} S. Pacetti^{28B,28C} X. Pan (潘祥)⁵⁵ Y. Pan (潘越)⁵⁷
 A. Pathak³⁴ P. Patteri^{28A} Y. P. Pei (裴宇鹏)^{71,58} M. Pelizaeus³ H. P. Peng (彭海平)^{71,58} Y. Y. Peng (彭云翊)^{38,k,1}
 K. Peters^{13,e} J. L. Ping (平加伦)⁴¹ R. G. Ping (平荣刚)^{1,63} S. Plura³⁵ V. Prasad³³ F. Z. Qi (齐法制)¹
 H. Qi (齐航)^{71,58} H. R. Qi (漆红荣)⁶¹ M. Qi (祁鸣)⁴² T. Y. Qi (齐天钰)^{12,g} S. Qian (钱森)^{1,58} W. B. Qian (钱文斌)⁶³
 C. F. Qiao (乔从丰)⁶³ X. K. Qiao (乔晓珂)⁸⁰ J. J. Qin (秦佳佳)⁷² L. Q. Qin (秦丽清)¹⁴ L. Y. Qin (秦龙宇)^{71,58}
 X. S. Qin (秦小帅)⁵⁰ Z. H. Qin (秦中华)^{1,58} J. F. Qiu (邱进发)¹ Z. H. Qu (屈子皓)⁷² C. F. Redmer³⁵
 K. J. Ren (任旷洁)³⁹ A. Rivetti^{74C} M. Rolo^{74C} G. Rong (荣刚)^{1,63} Ch. Rosner¹⁸ S. N. Ruan (阮氏宁)⁴³ N. Salone⁴⁴
 A. Sarantsev^{36,d} Y. Schelhaas³⁵ K. Schoenning⁷⁵ M. Scodreggio^{29A} K. Y. Shan (尚科羽)^{12,g} W. Shan (单葳)²⁴
 X. Y. Shan (单心钰)^{71,58} Z. J. Shang (尚子杰)^{38,k,1} J. F. Shangguan (上官剑锋)⁵⁵ L. G. Shao (邵立港)^{1,63}
 M. Shao (邵明)^{71,58} C. P. Shen (沈成平)^{12,g} H. F. Shen (沈宏飞)^{1,8} W. H. Shen (沈文涵)⁶³ X. Y. Shen (沈肖雁)^{1,63}
 B. A. Shi (施伯安)⁶³ H. Shi (史华)^{1,58} H. C. Shi (石煌超)^{71,58} J. L. Shi (石家磊)^{12,g} J. Y. Shi (石京燕)¹
 Q. Q. Shi (石勤强)⁵⁵ S. Y. Shi (史书宇)⁷² X. Shi (史欣)^{1,58} J. J. Song (宋娇娇)¹⁹ T. Z. Song (宋天资)⁵⁹
 W. M. Song (宋维民)^{34,1} Y. J. Song (宋宇镜)^{12,g} Y. X. Song (宋昀轩)^{46,h,n} S. Sosio^{74A,74C} S. Spataro^{74A,74C}
 F. Stieler³⁵ Y. J. Su (粟杨捷)⁶³ G. B. Sun (孙光豹)⁷⁶ G. X. Sun (孙功星)¹ H. Sun (孙昊)⁶³ H. K. Sun (孙浩凯)¹

J. F. Sun (孙俊峰)¹⁹ K. Sun (孙开)⁶¹ L. Sun (孙亮)⁷⁶ S. S. Sun (孙胜森)^{1,63} T. Sun^{51,f} W. Y. Sun (孙文玉)³⁴
 Y. Sun (孙源)⁹ Y. J. Sun (孙勇杰)^{71,58} Y. Z. Sun (孙永昭)¹ Z. Q. Sun (孙泽群)^{1,63} Z. T. Sun (孙振田)⁵⁰
 C. J. Tang (唐昌建)⁵⁴ G. Y. Tang (唐光毅)¹ J. Tang (唐健)⁵⁹ M. Tang (唐嘉骏)^{71,58} Y. A. Tang (唐迎澳)⁷⁶
 L. Y. Tao (陶璐燕)⁷² Q. T. Tao (陶秋田)^{25,i} M. Tat⁶⁹ J. X. Teng (滕佳秀)^{71,58} V. Thoren⁷⁵ W. H. Tian (田文辉)⁵⁹
 Y. Tian (田野)^{31,63} Z. F. Tian (田喆飞)⁷⁶ I. Uman^{62B} Y. Wan (万宇)⁵⁵ S. J. Wang (王少杰)⁵⁰ B. Wang (王斌)¹
 B. L. Wang (王滨龙)⁶³ Bo Wang (王博)^{71,58} D. Y. Wang (王大勇)^{46,h} F. Wang (王菲)⁷² H. J. Wang (王泓鉴)^{38,k,1}
 J. J. Wang (王家驹)⁷⁶ J. P. Wang (王吉鹏)⁵⁰ K. Wang (王科)^{1,58} L. L. Wang (王亮亮)¹ M. Wang (王萌)⁵⁰
 N. Y. Wang (王南洋)⁶³ S. Wang (王顺)^{12,g} S. Wang (王石)^{38,k,1} T. Wang (王婷)^{12,g} T. J. Wang (王腾蛟)⁴³
 W. Wang (王维)⁷² W. Wang (王为)⁵⁹ W. P. Wang (王维平)^{35,71,o} X. Wang (王轩)^{46,h} X. F. Wang (王雄飞)^{38,k,1}
 X. J. Wang (王希俊)³⁹ X. L. Wang (王小龙)^{12,g} X. N. Wang (王新南)¹ Y. Wang (王亦)⁶¹ Y. D. Wang (王雅迪)⁴⁵
 Y. F. Wang (王贻芳)^{1,58,63} Y. L. Wang (王艺龙)¹⁹ Y. N. Wang (王亚男)⁴⁵ Y. Q. Wang (王雨晴)¹
 Yaqian Wang (王亚乾)¹⁷ Yi Wang (王义)⁶¹ Z. Wang (王铮)^{1,58} Z. L. Wang (王治浪)⁷² Z. Y. Wang (王至勇)^{1,63}
 Ziyi Wang (王子一)⁶³ D. H. Wei (魏代会)¹⁴ F. Weidner⁶⁸ S. P. Wen (文硕频)¹ Y. R. Wen (温亚冉)³⁹ U. Wiedner³
 G. Wilkinson⁶⁹ M. Wolke⁷⁵ L. Wollenberg³ C. Wu (吴晨)³⁹ J. F. Wu (吴金飞)^{1,8} L. H. Wu (伍灵慧)¹
 L. J. Wu (吴连近)^{1,63} X. Wu (吴潇)^{12,g} X. H. Wu (伍雄浩)³⁴ Y. Wu (吴言)^{71,58} Y. H. Wu (吴业昊)⁵⁵
 Y. J. Wu (吴英杰)³¹ Z. Wu (吴智)^{1,58} L. Xia (夏磊)^{71,58} X. M. Xian (咸秀梅)³⁹ B. H. Xiang (向本后)^{1,63}
 T. Xiang (相腾)^{46,h} D. Xiao (肖栋)^{38,k,1} G. Y. Xiao (肖光延)⁴² S. Y. Xiao (肖素玉)¹ Y. L. Xiao (肖云龙)^{12,g}
 Z. J. Xiao (肖振军)⁴¹ C. Xie (谢陈)⁴² X. H. Xie (谢昕海)^{46,h} Y. Xie (谢勇)⁵⁰ Y. G. Xie (谢宇广)^{1,58}
 Y. H. Xie (谢跃红)⁶ Z. P. Xie (谢智鹏)^{71,58} T. Y. Xing (邢天宇)^{1,63} C. F. Xu^{1,63} C. J. Xu (许创杰)⁵⁹
 G. F. Xu (许国发)¹ H. Y. Xu (许皓月)^{66,2,p} M. Xu (徐明)^{71,58} Q. J. Xu (徐庆君)¹⁶ Q. N. Xu³⁰ W. Xu (许威)¹
 W. L. Xu (徐万伦)⁶⁶ X. P. Xu (徐新平)⁵⁵ Y. C. Xu (胥英超)⁷⁷ Z. P. Xu (许泽鹏)⁴² Z. S. Xu (许昭燊)⁶³
 F. Yan (严芳)^{12,g} L. Yan (严亮)^{12,g} W. B. Yan (鄢文标)^{71,58} W. C. Yan (闫文成)⁸⁰ X. Q. Yan (严薛强)¹
 H. J. Yang (杨海军)^{51,f} H. L. Yang (杨昊霖)³⁴ H. X. Yang (杨洪勋)¹ Tao Yang (杨涛)¹ Y. Yang (杨莹)^{12,g}
 Y. F. Yang (杨艳芳)⁴³ Y. X. Yang (杨逸翔)^{1,63} Yifan Yang (杨翊凡)^{1,63} Z. W. Yang (杨政武)^{38,k,1}
 Z. P. Yao (姚志鹏)⁵⁰ M. Ye (叶梅)^{1,58} M. H. Ye (叶铭汉)⁸ J. H. Yin (殷俊昊)¹ Z. Y. You (尤邦响)⁵⁹
 B. X. Yu (俞伯祥)^{1,58,63} C. X. Yu (喻纯旭)⁴³ G. Yu (余刚)^{1,63} J. S. Yu (俞洁晟)^{25,i} T. Yu (于涛)⁷²
 X. D. Yu (余旭东)^{46,h} Y. C. Yu (于勇超)⁸⁰ C. Z. Yuan (苑长征)^{1,63} J. Yuan (袁杰)⁴⁵ J. Yuan (袁菁)³⁴
 L. Yuan (袁丽)² S. C. Yuan (苑思成)¹ Y. Yuan (袁野)^{1,63} Z. Y. Yuan (袁朝阳)⁵⁹ C. X. Yue (岳崇兴)³⁹
 A. A. Zafar⁷³ F. R. Zeng (曾凡蕊)⁵⁰ S. H. Zeng (曾胜辉)⁷² X. Zeng (曾鑫)^{12,g} Y. Zeng (曾云)^{25,i}
 Y. J. Zeng (曾宇杰)⁵⁹ Y. J. Zeng (曾溢嘉)^{1,63} X. Y. Zhai (翟星晔)³⁴ Y. C. Zhai (翟云聪)⁵⁰ Y. H. Zhan (詹永华)⁵⁹
 A. Q. Zhang (张安庆)^{1,63} B. L. Zhang (张伯伦)^{1,63} B. X. Zhang (张丙新)¹ D. H. Zhang (张丹昊)⁴³
 G. Y. Zhang (张广义)¹⁹ H. Zhang (张豪)^{71,58} H. Zhang (张晗)⁸⁰ H. C. Zhang (张航畅)^{1,58,63} H. H. Zhang (张宏宏)³⁴
 H. H. Zhang (张宏浩)⁵⁹ H. Q. Zhang (张华桥)^{1,58,63} H. R. Zhang (张浩然)^{71,58} H. Y. Zhang (章红宇)^{1,58}
 J. Zhang (张晋)⁵⁹ J. Zhang (张进)⁸⁰ J. J. Zhang (张进军)⁵² J. L. Zhang (张杰磊)²⁰ J. Q. Zhang (张敬庆)⁴¹
 J. S. Zhang (张家声)^{12,g} J. W. Zhang (张家文)^{1,58,63} J. X. Zhang (张景旭)^{38,k,1} J. Y. Zhang (张建勇)¹
 J. Z. Zhang (张景芝)^{1,63} Jianyu Zhang (张剑宇)⁶³ L. M. Zhang (张黎明)⁶¹ Lei Zhang (张雷)⁴² P. Zhang (张鹏)^{1,63}
 Q. Y. Zhang (张秋岩)³⁴ R. Y. Zhang (张若愚)^{38,k,1} Shuihan Zhang (张水涵)^{1,63} Shulei Zhang (张书磊)^{25,i}
 X. D. Zhang (张小东)⁴⁵ X. M. Zhang (张晓梅)¹ X. Y. Zhang (张学尧)⁵⁰ Y. Zhang (张宇)⁷² Y. T. Zhang (张亚腾)⁸⁰
 Y. H. Zhang (张银鸿)^{1,58} Y. M. Zhang (张悦明)³⁹ Yan Zhang (张言)^{71,58} Yao Zhang (张瑶)¹ Z. D. Zhang (张正德)¹
 Z. H. Zhang (张泽恒)¹ Z. L. Zhang (张兆领)³⁴ Z. Y. Zhang (张振宇)⁷⁶ Z. Y. Zhang (张子羽)⁴³
 Z. Z. Zhang (张子扬)⁴⁵ G. Zhao (赵光)¹ J. Y. Zhao (赵静宜)^{1,63} J. Z. Zhao (赵京周)^{1,58} Lei Zhao (赵雷)^{71,58}
 Ling Zhao (赵玲)¹ M. G. Zhao (赵明刚)⁴³ N. Zhao (赵宁)⁷⁸ R. P. Zhao (赵若平)⁶³ S. J. Zhao (赵书俊)⁸⁰
 Y. B. Zhao (赵豫斌)^{1,58} Y. X. Zhao (赵宇翔)^{31,63} Z. G. Zhao (赵政国)^{71,58} A. Zhemchugov^{36,b} B. Zheng (郑波)⁷²
 B. M. Zheng (郑变敏)³⁴ J. P. Zheng (郑建平)^{1,58} W. J. Zheng (郑文静)^{1,63} Y. H. Zheng (郑阳恒)⁶³ B. Zhong (钟彬)⁴¹
 X. Zhong (钟鑫)⁵⁹ H. Zhou (周航)⁵⁰ J. Y. Zhou (周佳莹)³⁴ L. P. Zhou (周利鹏)^{1,63} S. Zhou (周帅)⁶
 X. Zhou (周详)⁷⁶ X. K. Zhou (周晓康)⁶ X. R. Zhou (周小蓉)^{71,58} X. Y. Zhou (周兴玉)³⁹ Y. Z. Zhou (周祎卓)^{12,g}

J. Zhu (朱江)⁴³ K. Zhu (朱凯)¹ K. J. Zhu (朱科军)^{1,58,63} K. S. Zhu (朱康帅)^{12,g} L. Zhu (朱林)³⁴
 L. X. Zhu (朱琳萱)⁶³ S. H. Zhu (朱世海)⁷⁰ S. Q. Zhu (朱仕强)⁴² T. J. Zhu (朱腾蛟)^{12,g} W. D. Zhu (朱稳定)⁴¹
 Y. C. Zhu (朱莹春)^{71,58} Z. A. Zhu (朱自安)^{1,63} J. H. Zou (邹佳恒)¹ J. Zu (祖健)^{71,58}

(BESIII Collaboration)

- ¹Institute of High Energy Physics, Beijing 100049, China
²Beihang University, Beijing 100191, China
³Bochum Ruhr-University, D-44780 Bochum, Germany
⁴Budker Institute of Nuclear Physics SB RAS (BINP), Novosibirsk 630090, Russia
⁵Carnegie Mellon University, Pittsburgh, Pennsylvania 15213, USA
⁶Central China Normal University, Wuhan 430079, China
⁷Central South University, Changsha 410083, China
⁸China Center of Advanced Science and Technology, Beijing 100190, China
⁹China University of Geosciences, Wuhan 430074, China
¹⁰Chung-Ang University, Seoul, 06974, Republic of Korea
¹¹COMSATS University Islamabad, Lahore Campus, Defence Road, Off Raiwind Road, 54000 Lahore, Pakistan
¹²Fudan University, Shanghai 200433, China
¹³GSI Helmholtzcentre for Heavy Ion Research GmbH, D-64291 Darmstadt, Germany
¹⁴Guangxi Normal University, Guilin 541004, China
¹⁵Guangxi University, Nanning 530004, China
¹⁶Hangzhou Normal University, Hangzhou 310036, China
¹⁷Hebei University, Baoding 071002, China
¹⁸Helmholtz Institute Mainz, Staudinger Weg 18, D-55099 Mainz, Germany
¹⁹Henan Normal University, Xinxiang 453007, China
²⁰Henan University, Kaifeng 475004, China
²¹Henan University of Science and Technology, Luoyang 471003, China
²²Henan University of Technology, Zhengzhou 450001, China
²³Huangshan College, Huangshan 245000, China
²⁴Hunan Normal University, Changsha 410081, China
²⁵Hunan University, Changsha 410082, China
²⁶Indian Institute of Technology Madras, Chennai 600036, India
²⁷Indiana University, Bloomington, Indiana 47405, USA
²⁸INFN Laboratori Nazionali di Frascati, (A)INFN Laboratori Nazionali di Frascati, I-00044, Frascati, Italy; (B)INFN Sezione di Perugia, I-06100, Perugia, Italy; (C)University of Perugia, I-06100, Perugia, Italy
²⁹INFN Sezione di Ferrara, (A)INFN Sezione di Ferrara, I-44122, Ferrara, Italy; (B)University of Ferrara, I-44122, Ferrara, Italy
³⁰Inner Mongolia University, Hohhot 010021, China
³¹Institute of Modern Physics, Lanzhou 730000, China
³²Institute of Physics and Technology, Peace Avenue 54B, Ulaanbaatar 13330, Mongolia
³³Instituto de Alta Investigación, Universidad de Tarapacá, Casilla 7D, Arica 1000000, Chile
³⁴Jilin University, Changchun 130012, China
³⁵Johannes Gutenberg University of Mainz, Johann-Joachim-Becher-Weg 45, D-55099 Mainz, Germany
³⁶Joint Institute for Nuclear Research, 141980 Dubna, Moscow region, Russia
³⁷Justus-Liebig-Universität Giessen, II. Physikalisches Institut, Heinrich-Buff-Ring 16, D-35392 Giessen, Germany
³⁸Lanzhou University, Lanzhou 730000, China
³⁹Liaoning Normal University, Dalian 116029, China
⁴⁰Liaoning University, Shenyang 110036, China
⁴¹Nanjing Normal University, Nanjing 210023, China
⁴²Nanjing University, Nanjing 210093, China
⁴³Nankai University, Tianjin 300071, China
⁴⁴National Centre for Nuclear Research, Warsaw 02-093, Poland
⁴⁵North China Electric Power University, Beijing 102206, China
⁴⁶Peking University, Beijing 100871, China
⁴⁷Qufu Normal University, Qufu 273165, China
⁴⁸Renmin University of China, Beijing 100872, China
⁴⁹Shandong Normal University, Jinan 250014, China
⁵⁰Shandong University, Jinan 250100, China
⁵¹Shanghai Jiao Tong University, Shanghai 200240, China
⁵²Shanxi Normal University, Linfen 041004, China
⁵³Shanxi University, Taiyuan 030006, China
⁵⁴Sichuan University, Chengdu 610064, China
⁵⁵Soochow University, Suzhou 215006, China
⁵⁶South China Normal University, Guangzhou 510006, China
⁵⁷Southeast University, Nanjing 211100, China
⁵⁸State Key Laboratory of Particle Detection and Electronics, Beijing 100049, Hefei 230026, China
⁵⁹Sun Yat-Sen University, Guangzhou 510275, China
⁶⁰Suranaree University of Technology, University Avenue 111, Nakhon Ratchasima 30000, Thailand
⁶¹Tsinghua University, Beijing 100084, China

⁶²Turkish Accelerator Center Particle Factory Group, (A)Istinye University, 34010, Istanbul, Turkey; (B)Near East University, Nicosia, North Cyprus, 99138, Mersin 10, Turkey

⁶³University of Chinese Academy of Sciences, Beijing 100049, China

⁶⁴University of Groningen, NL-9747 AA Groningen, The Netherlands

⁶⁵University of Hawaii, Honolulu, Hawaii 96822, USA

⁶⁶University of Jinan, Jinan 250022, China

⁶⁷University of Manchester, Oxford Road, Manchester, M13 9PL, United Kingdom

⁶⁸University of Muenster, Wilhelm-Klemm-Strasse 9, 48149 Muenster, Germany

⁶⁹University of Oxford, Keble Road, Oxford OX13RH, United Kingdom

⁷⁰University of Science and Technology Liaoning, Anshan 114051, China

⁷¹University of Science and Technology of China, Hefei 230026, China

⁷²University of South China, Hengyang 421001, China

⁷³University of the Punjab, Lahore-54590, Pakistan

⁷⁴University of Turin and INFN, (A)University of Turin, I-10125, Turin, Italy; (B)University of Eastern Piedmont, I-15121, Alessandria, Italy; (C)INFN, I-10125, Turin, Italy

⁷⁵Uppsala University, Box 516, SE-75120 Uppsala, Sweden

⁷⁶Wuhan University, Wuhan 430072, China

⁷⁷Yantai University, Yantai 264005, China

⁷⁸Yunnan University, Kunming 650500, China

⁷⁹Zhejiang University, Hangzhou 310027, China

⁸⁰Zhengzhou University, Zhengzhou 450001, China

^aDeceased

^bAlso at the Moscow Institute of Physics and Technology, Moscow 141700, Russia

^cAlso at the Novosibirsk State University, Novosibirsk, 630090, Russia

^dAlso at the NRC "Kurchatov Institute", PNPI, 188300, Gatchina, Russia

^eAlso at Goethe University Frankfurt, 60323 Frankfurt am Main, Germany

^fAlso at Key Laboratory for Particle Physics, Astrophysics and Cosmology, Ministry of Education; Shanghai Key Laboratory for Particle Physics and Cosmology; Institute of Nuclear and Particle Physics, Shanghai 200240, China

^gAlso at Key Laboratory of Nuclear Physics and Ion-beam Application (MOE) and Institute of Modern Physics, Fudan University, Shanghai 200443, China

^hAlso at State Key Laboratory of Nuclear Physics and Technology, Peking University, Beijing 100871, China

ⁱAlso at School of Physics and Electronics, Hunan University, Changsha 410082, China

^jAlso at Guangdong Provincial Key Laboratory of Nuclear Science, Institute of Quantum Matter, South China Normal University, Guangzhou 510006, China

^kAlso at MOE Frontiers Science Center for Rare Isotopes, Lanzhou University, Lanzhou 730000, China

^lAlso at Lanzhou Center for Theoretical Physics, Lanzhou University, Lanzhou 730000, China

^mAlso at the Department of Mathematical Sciences, IBA, Karachi 75270, Pakistan

ⁿAlso at Ecole Polytechnique Federale de Lausanne (EPFL), CH-1015 Lausanne, Switzerland

^oAlso at Helmholtz Institute Mainz, Staudinger Weg 18, D-55099 Mainz, Germany

^pAlso at School of Physics, Beihang University, Beijing 100191, China

Abstract: The number of $\psi(3686)$ events collected by the BESIII detector during the 2021 run period is determined to be $(2259.3 \pm 11.1) \times 10^6$ by counting inclusive $\psi(3686)$ hadronic events. The uncertainty is systematic and the statistical uncertainty is negligible. Meanwhile, the numbers of $\psi(3686)$ events collected during the 2009 and 2012 run periods are updated to be $(107.7 \pm 0.6) \times 10^6$ and $(345.4 \pm 2.6) \times 10^6$, respectively. Both numbers are consistent with the previous measurements within one standard deviation. The total number of $\psi(3686)$ events in the three data samples is $(2712.4 \pm 14.3) \times 10^6$.

Keywords: $\psi(3686)$, inclusive process, Hadronic events, BESIII detector

DOI: 10.1088/1674-1137/ad595b

I. INTRODUCTION

In 2009, 2012, and 2021, the BESIII experiment accumulated the world's largest $\psi(3686)$ data sample produced in electron-positron collisions, thereby providing an excellent platform to precisely study the transitions and decays of the $\psi(3686)$ and its daughter charmonium states, including the χ_{cJ} , h_c , and η_c , and to search for rare decays with physics beyond the Standard Model. The number of $\psi(3686)$ events, $N_{\psi(3686)}$, is a basic input parameter, and its precision has a direct impact on the accu-

acy of these measurements.

In this paper, we determine the number of $\psi(3686)$ events by using inclusive $\psi(3686)$ hadronic decays, where the branching fraction of $\psi(3686) \rightarrow \text{hadrons}$ is known to be $(97.85 \pm 0.13)\%$ [1–3]. The nonresonant background yield under the $\psi(3686)$ peak is evaluated by analyzing the two off-resonance data samples taken in 2009 and 2021 at a center-of-mass (c.m.) energy $E_{\text{cm}} = 3.65$ GeV. The same method of background estimation was successfully used in our previous measurement of the numbers of $\psi(3686)$ events in the data samples collected

in 2009 and 2012 [4].

II. BEPCII AND BESIII DETECTOR

BEPCII [5] is a double-ring e^+e^- collider in the center-of-mass energy range from 2.0 to 4.95 GeV which has reached a peak luminosity of $1 \times 10^{33} \text{ cm}^{-2}\text{s}^{-1}$ at $\sqrt{s} = 3.773$ GeV. The cylindrical core of the BESIII detector [5] consists of a helium-based multilayer drift chamber (MDC), a plastic scintillator time-of-flight (TOF) system, and a CsI(Tl) electromagnetic calorimeter (EMC), which are all enclosed in a superconducting solenoid magnet with a field strength of 1.0 T (0.9 T in 2012). The solenoid is supported by an octagonal flux-return yoke with resistive plate counter modules interleaved with steel as a muon identifier. The acceptance for charged particles and photons is 93% over the 4π stereo angle. The charged-particle momentum resolution at 1 GeV/c is 0.5%, and the photon energy resolution at 1 GeV is 2.5% (5%) in the barrel (end-caps) of the EMC. The time resolution in the TOF barrel region is 68 ps, while that in the end cap region was 110 ps. The end cap TOF system was upgraded in 2015 using multigap resistive plate chamber technology, providing a time resolution of 60 ps. The MDC encountered the Malter effect due to cathode aging during $\psi(3686)$ data taking in 2012. This effect was suppressed by mixing about 0.2% water vapor into the MDC operating gas [6] and can be well modeled by Monte Carlo (MC) simulation. The other sub-detectors worked well during 2009, 2012, and 2021 operation.

The BESIII detector is modeled with a MC simulation based on GEANT4 [7]. The $\psi(3686)$ produced in the electron-positron collisions are simulated with the generator KKMC [8], which includes the beam energy spread according to the measurement of BEPCII and the effect of initial state radiation (ISR). The known decay modes of the $\psi(3686)$ are generated with EVTGEN [9] according to the branching fractions from the Particle Data Group [3], while the remaining unknown decays are simulated using the LUNDCHARM model [10]. The MC events are mixed with randomly triggered events (non-physical events from collision) from data to take into account possible effects from beam-related backgrounds, cosmic rays, and electronic noise.

III. EVENT SELECTION

The data collected at the $\psi(3686)$ peak includes several different processes, *i.e.*, $\psi(3686) \rightarrow \text{hadrons}$, $\psi(3686) \rightarrow \ell^+\ell^-$ ($\ell = e, \mu$ or τ), ISR return to J/ψ , and nonresonant background including $e^+e^- \rightarrow \gamma^* \rightarrow \text{hadrons}$ (qq ($q = u, d, s$)), $e^+e^- \rightarrow \ell^+\ell^-$, and $e^+e^- \rightarrow e^+e^- + X$ ($X = \text{hadrons}, \ell^+\ell^-$). The data also contains non-collision events, *e.g.*, cosmic rays, beam-associated backgrounds, and electronic noise.

To separate the candidate events for $\psi(3686) \rightarrow \text{hadrons}$ from backgrounds, we require that there is at least one good charged track candidate in each event. The charged tracks are required to be within 10 cm from the Interaction Point (IP) in the z axis, within 1 cm in the perpendicular plane and within a polar angle range of $|\cos\theta| < 0.93$ in the MDC, where θ is the angle measured relative to the z axis. Photons reconstructed in the EMC barrel region ($|\cos\theta| < 0.80$) must have a minimum energy of 25 MeV, while those in the end-caps ($0.86 < |\cos\theta| < 0.92$) must have an energy of at least 50 MeV. The photons in the polar angle range between the barrel and end-caps are excluded due to the poor resolution. A requirement of the EMC cluster timing [0, 700] ns is applied to suppress electronic noise and energy deposits unrelated to the event.

The selected hadronic events are classified into three categories according to the multiplicity of good charged tracks (N_{good}), *i.e.*, type-I ($N_{\text{good}} = 1$), type-II ($N_{\text{good}} = 2$) and type-III ($N_{\text{good}} > 2$). For the type-III events, no further selection criteria are required.

For the type-II events, the momenta of the two charged tracks (p_1 and p_2) are required to be less than 1.7 GeV/c and the opening angle between them (Δ_α) is required to be less than 176° to suppress Bhabha ($e^+e^- \rightarrow e^+e^-$) and dimuon ($e^+e^- \rightarrow \mu^+\mu^-$) backgrounds. Figure 1 shows the distributions of p_2 versus p_1 and Δ_α for the type-II events from the simulated Bhabha and inclusive $\psi(3686)$ MC samples. Furthermore, a requirement of $E_{\text{visible}}/E_{\text{cm}} > 0.4$ is applied to suppress the low energy background (LEB), which may comprise $e^+e^- \rightarrow e^+e^- + X$, double ISR events ($e^+e^- \rightarrow \gamma_{\text{ISR}}\gamma_{\text{ISR}}X$), *etc.* Here, E_{visible} is the visible energy which is the sum of the energy of all the charged tracks calculated with the track momentum assuming the tracks to be pions and all the neutral showers. Figure 2 (left) shows the $E_{\text{visible}}/E_{\text{cm}}$ distributions of the type-II events for the $\psi(3686)$ data and inclusive MC samples. The visible excess in inclusive MC at low energy is from $\psi(3686) \rightarrow \pi^+\pi^-J/\psi$, $J/\psi \rightarrow e^+e^-, \mu^+\mu^-$ where the lepton pair is missing. Unless noted, in all plots, the points with error bars are the $\psi(3686)$ data sample collected in 2021, and the histogram is the corresponding inclusive MC sample.

For the type-I events, at least two photons are required in the event. Compared to those events with high charged track multiplicity, the type-I sample has more background according to the vertex distribution of the charged tracks. Thus, a neutral hadron π^0 candidate is required to improve the suppression of background events [4], where the π^0 candidate is reconstructed from a $\gamma\gamma$ pair. Within each event, only the $\gamma\gamma$ candidate with invariant mass closest to the π^0 nominal mass and satisfying $|M_{\gamma\gamma} - M_{\pi^0}| < 0.015 \text{ GeV}/c^2$ is kept for further analysis. Figure 3 shows the $M_{\gamma\gamma}$ distribution of the selected π^0 candidates for type-I events. With the above selection cri-

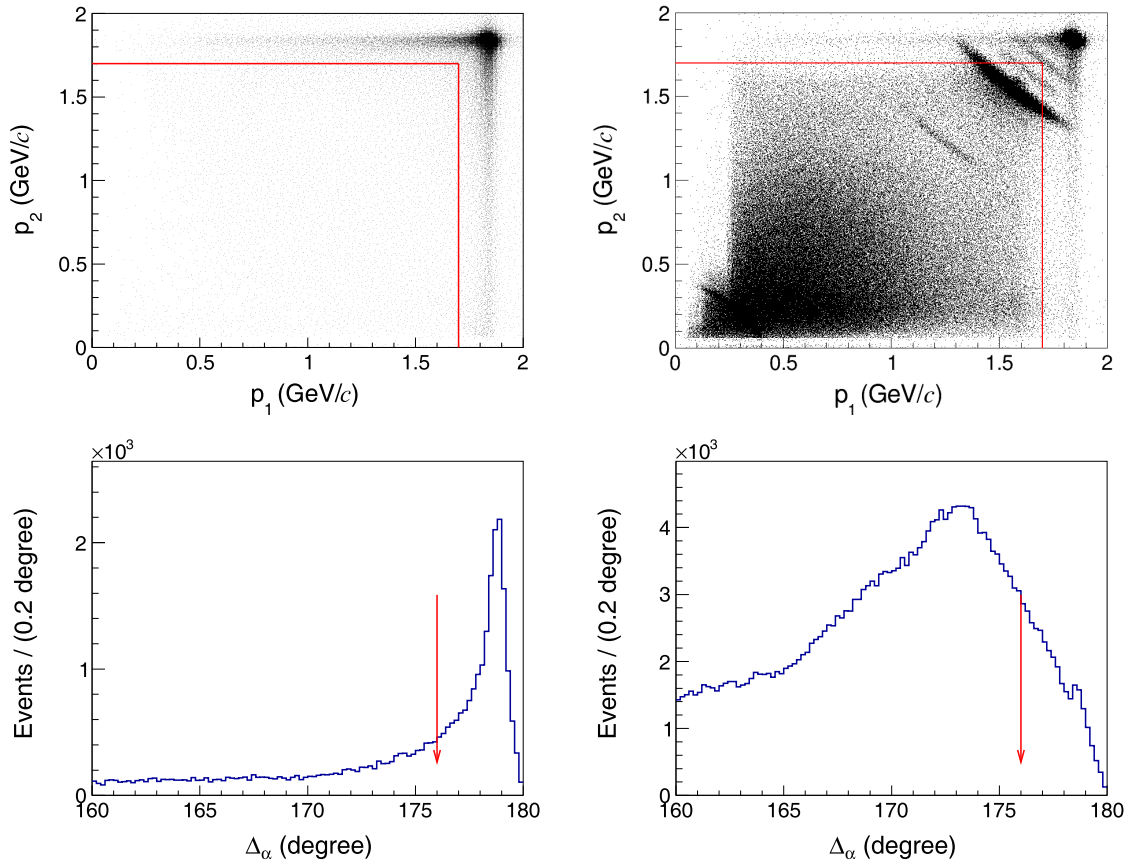


Fig. 1. (color online) Distributions of p_2 versus p_1 (top) and Δ_α (bottom) for the type-II events from the (left) simulated Bhabha and (right) $\psi(3686)$ inclusive MC samples. The events satisfying $p < 1.7$ GeV/ c and $\Delta_\alpha < 176^\circ$ are kept for further analysis. In the top-right plot, the event accumulation in the top-right corner comes from $\psi(3686) \rightarrow e^+e^-, \mu^+\mu^-$, while the different event bands come from $\psi(3686) \rightarrow \text{neutral} + J/\psi, J/\psi \rightarrow e^+e^-, \mu^+\mu^-$, etc., and the event band in the bottom-left comes from $\psi(3686) \rightarrow \pi^+\pi^-J/\psi, J/\psi \rightarrow e^+e^-, \mu^+\mu^-$ where the lepton pair is missing.

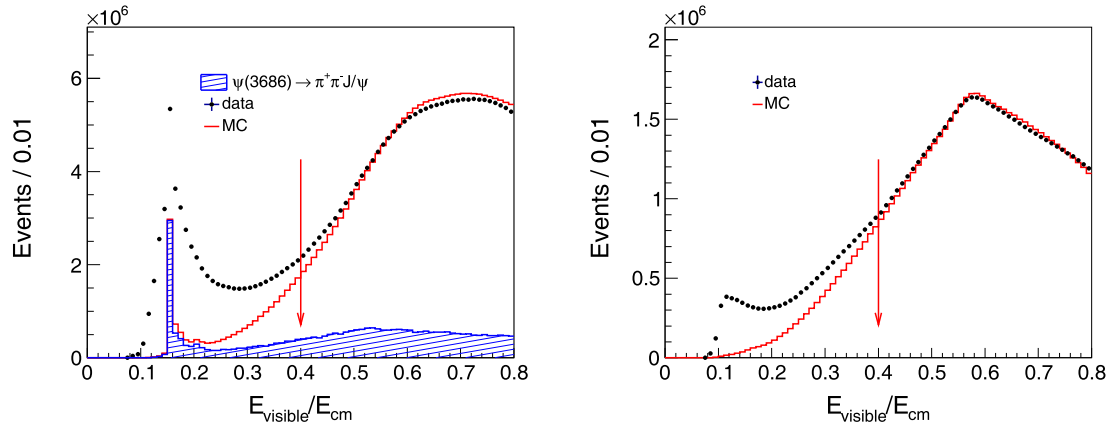


Fig. 2. (color online) Distributions of $E_{\text{visible}}/E_{\text{cm}}$ for the type-II (left) and type-I (right) events of the $\psi(3686)$ data and inclusive MC samples. The MC distributions have been scaled to data by using events with $E_{\text{visible}}/E_{\text{cm}} > 0.4$. The events lying above the red arrows are kept for further analysis.

teria, the corresponding $E_{\text{visible}}/E_{\text{cm}}$ distributions of the candidate events for the $\psi(3686)$ data and inclusive MC samples are shown in Fig. 2(right). An additional requirement of $E_{\text{visible}}/E_{\text{cm}} > 0.4$ is also used to suppress the LEB

events.

The signal yield of $e^+e^- \rightarrow \text{hadrons}$ is obtained by examining the event vertex distribution V_Z . For type-II and type-III events, the V_Z is the event vertex fit position,

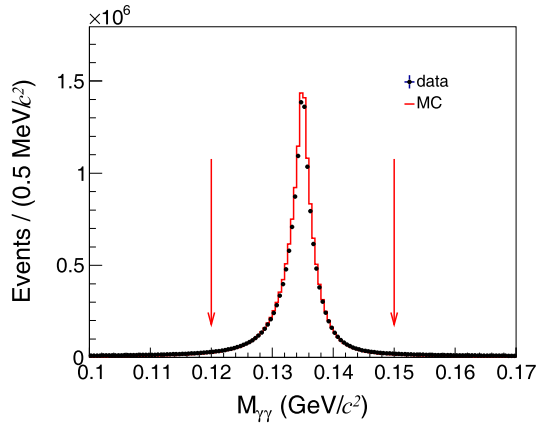


Fig. 3. (color online) Distribution of $M_{\gamma\gamma}$ for the π^0 candidates from the type-I events. The region within the pair of red arrows is the π^0 signal window.

while for type-I events, the V_Z is the defined one for single track, *i.e.*, the distance to IP in the z direction. **Figure 4** shows the distributions of V_Z for $\psi(3686)$ and off-resonance data samples. The region $|V_Z| < 4$ cm is regarded as the signal region, and the region $6 < |V_Z| < 10$ cm is taken as the sideband region. Events in the sideband region are mainly from non-collision background events. The number of observed hadronic events (N^{obs}) is determined by

$$N^{\text{obs}} = N_{\text{signal}} - N_{\text{sideband}}, \quad (1)$$

where N_{signal} and N_{sideband} are the numbers of events in the signal and sideband regions, respectively.

IV. BACKGROUND ANALYSIS

Following our previous measurement [4], the number of remaining $q\bar{q}$ background events is estimated using the

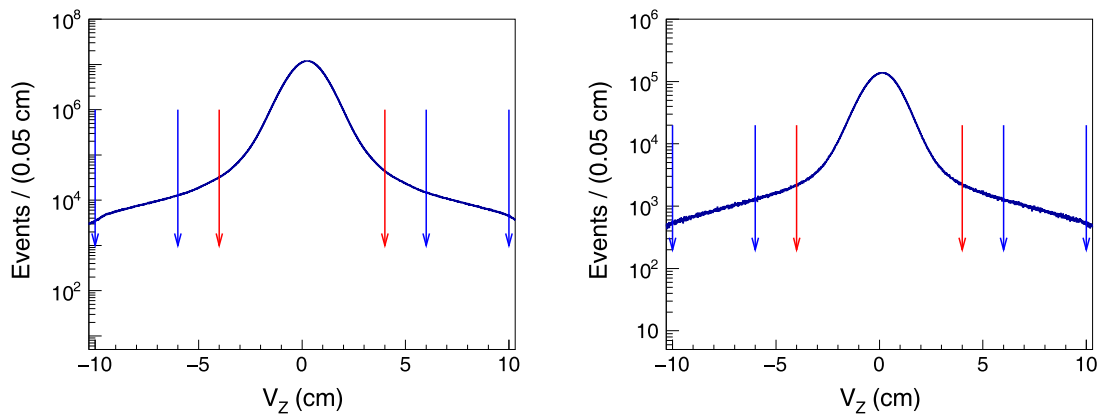


Fig. 4. (color online) The distributions of V_Z for the accepted hadronic events of the (left) $\psi(3686)$ data and (right) off-resonance data. The region within the pair of red arrows is the signal region, while the regions within the two pairs of blue arrows are the sideband regions.

off-resonance data sample benefiting from the small difference in the c.m. energies, where one expects the $q\bar{q}$ background is comparable so that can be used to estimate the background in the energy of $\psi(3686)$. We apply the same approach to determine the yields of collision events for the off-resonance data samples, then estimate the contribution at the $\psi(3686)$ resonance after scaling by integrated luminosity. Similarly, the contributions from the ISR return to J/ψ are estimated by the same method as above. The connection between two energy points can be expressed by a scaling factor, f , determined from the integrated luminosity multiplied by $1/s$ to account for the energy dependence of the cross section. This can be done since the dominant backgrounds come from the Bhabha and dimuon processes at the leading-order contribution [11]. The scale factor is

$$f = \frac{\mathcal{L}_{\psi(3686)}}{\mathcal{L}_{\text{off-res}}} \cdot \frac{3.65^2}{3.686^2}, \quad (2)$$

where $\mathcal{L}_{\psi(3686)}$ and $\mathcal{L}_{\text{off-res}}$ are the integrated luminosities of the $\psi(3686)$ data and off-resonance data samples, and 3.686^2 and 3.65^2 are the corresponding squares of c.m. energies, respectively.

The integrated luminosities at different energy points are determined using Bhabha events [12] with the following selection criteria. The number of charged tracks is required to be equal to two with net charge zero. Each track must have energy deposited in the EMC between 1.0 GeV and 2.5 GeV and a momentum less than $0.5 \times E_{\text{cm}} + 0.3$ GeV. Furthermore, the sum of the momenta of the positron and electron must be greater than $0.9 \times E_{\text{cm}}$. The cosine of the polar angle (θ) for each track is required to be within $|\cos\theta| < 0.8$ and their ϕ angles must satisfy $5^\circ < |\phi_1 - \phi_2| - 180^\circ < 40^\circ$. The luminosities of the $\psi(3686)$ and off-resonance data samples taken in 2021 are 3208.5 pb^{-1} and 401.0 pb^{-1} , with uncertainties of about

1%, respectively.

To test if the interference between Bhabha events and $\psi(3686) \rightarrow e^+e^-$ events affects the luminosity measurement, we examine the integrated luminosities of the $\psi(3686)$ data samples using $e^+e^- \rightarrow \gamma\gamma$ events with the following selection criteria. The number of showers is required to be greater than or equal to two with no candidate charged tracks. Each shower must have deposited energy in the EMC between 1.0 GeV and 2.5 GeV. The cosine of the polar angle (θ) for each shower is required to be within $|\cos\theta| < 0.8$. The two most energetic showers are required to be back to back ($||\theta_1 - 90^\circ| - |\theta_2 - 90^\circ|| < 10^\circ$) and with ϕ angles $||\phi_1 - \phi_2| - 180^\circ| < 2^\circ$. The difference of the measured luminosities is less than 0.1%.

The integrated luminosities of the two off-resonance data samples collected at $E_{\text{cm}}=3.65$ GeV in 2009 and 2021 are 44.5 and 401.0 pb^{-1} , respectively. The former one is used to estimate the continuum contribution of the 2009 $\psi(3686)$ data sample, and the latter one is used to estimate the continuum contribution of the 2012 and 2021 $\psi(3686)$ data samples. The integrated luminosities of the 2009, 2012, and 2021 $\psi(3686)$ data samples are 161.6, 506.9, and 3208.5 pb^{-1} , respectively, with scaling factors f of 3.56, 1.24, and 7.85, respectively. The systematic uncertainties of the luminosities for the two c.m. energies almost cancel when calculating the scaling factors due to the small energy difference.

The cross sections for $e^+e^- \rightarrow \tau^+\tau^-$ are calculated to be 1.84 and 2.14 nb at $E_{\text{cm}} = 3.65$ GeV and 3.686 GeV, respectively. Since the above energy points are close to the $\tau^+\tau^-$ mass threshold, the production cross section does not follow a $1/s$ distribution. Thus, only part of the $e^+e^- \rightarrow \tau^+\tau^-$ background events is included in the off-resonance data samples. To subtract the full background from $e^+e^- \rightarrow \tau^+\tau^-$, we estimate the remaining contribution, $N_{\tau^+\tau^-}^{\text{uncanceled}}$, using the detection efficiency from the MC simulation, the cross section difference at the two c.m. energy points, and the luminosity at the $\psi(3686)$

peak. The estimated residual $e^+e^- \rightarrow \tau^+\tau^-$ background yields are shown in Table 1.

The cross section from the ISR return to J/ψ is also found to slightly violate the $1/s$ distribution. However, the corrected cross section difference for this process at the $\psi(3686)$ peak is about 0.1 nb, which is negligible if compared to the total observed cross section of $\psi(3686) \rightarrow \text{hadrons}$, ~ 700 nb.

A small fraction of $\psi(3686) \rightarrow \ell^+\ell^-$ events survives the event selection. Since their effect has been considered in the detection efficiency, no further subtraction is made.

Figure 5 shows the comparisons of the distributions of $\cos\theta$, $E_{\text{visible}}/E_{\text{cm}}$, N_{good} , and photon multiplicity (N_γ) after background subtraction between data and MC simulation, and a reasonable data-MC agreement is observed. Table 1 summarizes the numbers of the observed hadronic events for different N_{good} requirements of $\psi(3686)$ data ($N_{\psi(3686)}^{\text{obs}}$) and off-resonance data ($N_{\text{off-res}}^{\text{obs}}$). The detection efficiencies of $\psi(3686) \rightarrow \text{hadrons}$ are determined with 2.3 billion $\psi(3686)$ inclusive MC events, where the branching fraction of $\psi(3686) \rightarrow \text{hadrons}$ is included in the efficiency.

V. NUMERICAL RESULTS

With the numbers listed in Table 1, we determine the number of $\psi(3686)$ events using

$$N_{\psi(3686)} = \frac{N_{\psi(3686)}^{\text{obs}} - f \cdot N_{\text{off-res}}^{\text{obs}} - N_{\tau^+\tau^-}^{\text{uncanceled}}}{\epsilon}. \quad (3)$$

The obtained numerical results for $N_{\psi(3686)}$ with different N_{good} requirements are slightly different with each other, mainly due to the imperfect simulation of the charged track multiplicity. To obtain a more accurate $N_{\psi(3686)}$, an unfolding method is employed based on an efficiency matrix determined from the $\psi(3686)$ inclusive

Table 1. Number of hadronic events $N_{\psi(3686)}^{\text{obs}}$ in the $\psi(3686)$ data, separately for different requirements on the number of good tracks N_{good} , where $N_{\psi(3686)}^{\text{obs}}$ is the number of hadronic events observed in the $\psi(3686)$ data, f is the scaling factor, $N_{\text{off-res}}^{\text{obs}}$ is the number of hadronic events observed in the off-resonance data, $N_{\tau^+\tau^-}^{\text{uncanceled}}$ is the number of remaining $e^+e^- \rightarrow \tau^+\tau^-$ events after subtracting the normalized off-resonance data, ϵ is the detection efficiency, and $N_{\psi(3686)}$ is the determined number of $\psi(3686)$ events. The statistical uncertainties are expected to be negligible.

Multiplicity	$N_{\text{good}} \geq 1$			$N_{\text{good}} \geq 2$			$N_{\text{good}} \geq 3$		
	Year	2009	2012	2021	2009	2012	2021	2009	2012
$N_{\psi(3686)}^{\text{obs}} (10^6)$	107.98	345.14	2246.93	104.77	333.79	2172.16	83.36	264.57	1722.56
f	3.56	1.24	7.85	3.56	1.24	7.85	3.56	1.24	7.85
$N_{\text{off-res}}^{\text{obs}} (10^6)$	2.05	18.18	18.18	1.99	17.65	17.65	0.75	6.51	6.51
$N_{\tau^+\tau^-}^{\text{uncanceled}} (10^6)$	0.04	0.13	0.80	0.04	0.12	0.76	0.01	0.03	0.22
ϵ (%)	93.21	92.83	92.86	90.42	89.65	89.86	74.69	73.39	73.85
$N_{\psi(3686)} (10^6)$	107.96	347.36	2265.08	107.99	347.75	2262.32	108.03	349.46	2262.94

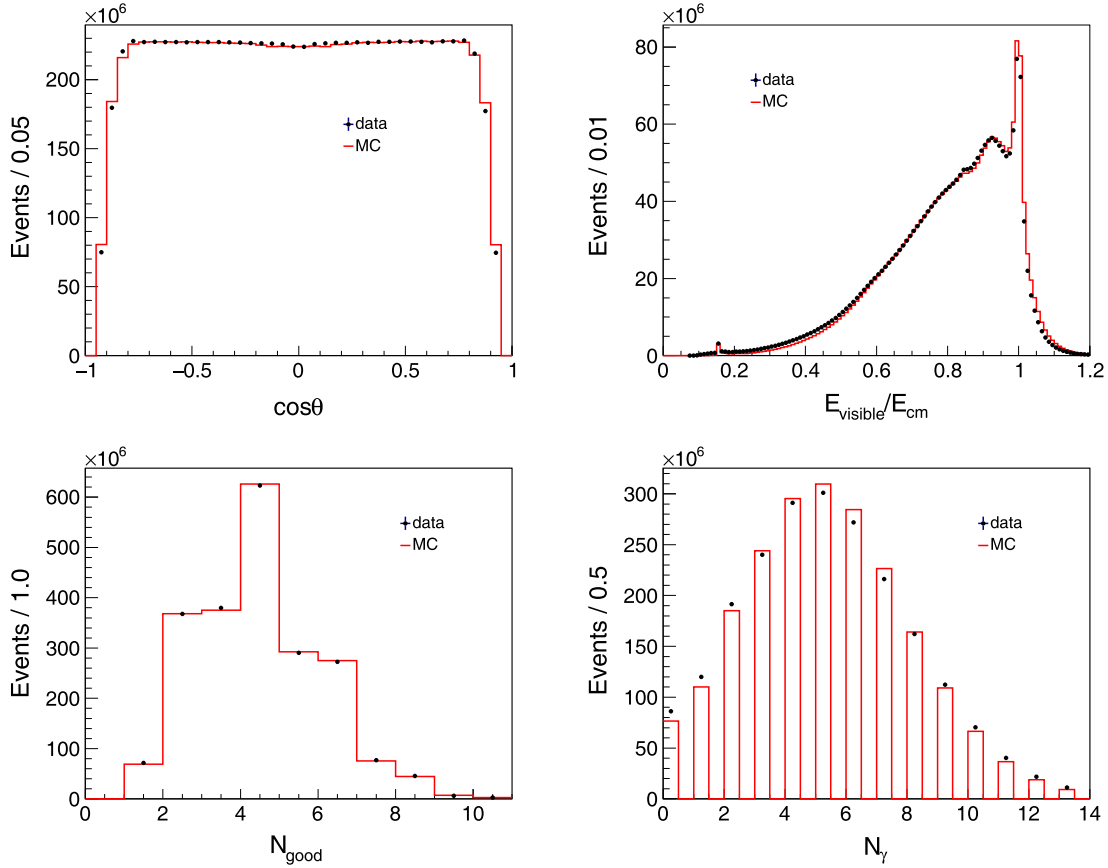


Fig. 5. (color online) Comparisons of the distributions of (top-left) $\cos\theta$, (top-right) $E_{\text{visible}}/E_{\text{cm}}$, (bottom-left) N_{good} , and (bottom-right) N_{γ} between $\psi(3686)$ data and inclusive MC samples after background subtraction.

MC sample. In practice, there are even numbers of charged tracks generated in an event due to charge conservation, while any number of charged tracks can be observed due to the reconstruction efficiency and backgrounds. Therefore, the true multiplicities of charged tracks of the data sample is estimated from the observed multiplicities of charged tracks and the efficiency matrix by minimizing the χ^2 , defined as

$$\chi^2 = \sum_{i=0}^{10} \frac{(N_i^{\text{obs}} - \sum_{j=0}^{10} \epsilon_{ij} \cdot N_j)^2}{N_i^{\text{obs}}}, \quad (4)$$

where the values N_i^{obs} ($i = 0, 1, 2, \dots$) are the observed multiplicities of charged tracks in the data sample corresponding to the distribution in Fig. 5 (bottom-left, the points with error bars), the matrix elements ϵ_{ij} represent the probability to observe i charged tracks for an event with j actual charged tracks, and the values N_j ($j = 0, 2, 4, \dots$) are the true multiplicities of charged tracks in the data sample. They are free parameters in the fit. For simplicity, the events with ten or more charged tracks are combined in the number N_{10} . The $N_{\psi(3686)}$ is calculated by summing over all the obtained N_j . The results are

107.7×10^6 , 345.4×10^6 and 2259.3×10^6 for the 2009, 2012 and 2021 data samples, respectively.

VI. SYSTEMATIC UNCERTAINTIES

The systematic uncertainties in the $N_{\psi(3686)}$ measurement from different sources are described below and listed in Table 2.

A. Polar angle of charged tracks

The polar angles of charged tracks are required to satisfy $|\cos\theta| < 0.93$. To estimate the relevant systematic uncertainty, we redo the measurement with an alternative requirement of $|\cos\theta| < 0.8$. The difference in the measured number of $\psi(3686)$ events is taken as the systematic uncertainty.

B. Tracking efficiency

The systematic uncertainties due to the tracking efficiency for both the 2009 and 2012 data samples have been found to be negligible based on various studies [4]. Therefore, the associated systematic uncertainty for the 2021 data sample is also ignored.

Table 2. Relative systematic uncertainties (%) in the determination of the number of $\psi(3686)$ events.

Source	2009	2012	2021
Polar angle of charged track	0.25	0.20	0.22
Tracking efficiency	negligible	negligible	negligible
Momentum and opening angle	0.20	0.26	0.26
LEB contamination	0.02	0.04	0.12
Extraction method of N^{obs}	0.16	0.16	0.03
Vertex requirement	0.13	0.08	0.07
Scaling factor (f)	negligible	negligible	negligible
π^0 mass requirement	negligible	0.01	0.05
Missing $N_{\text{good}} = 0$ hadronic events	0.38	0.31	0.11
Charged track multiplicity	0.24	0.56	0.26
MC modeling	negligible	negligible	negligible
Trigger efficiency	negligible	negligible	negligible
$\mathcal{B}(\psi(3686) \rightarrow \text{hadrons})$	0.13	0.13	0.13
Total	0.60	0.75	0.49

C. Momentum and opening angle

To estimate the systematic uncertainty due to the requirement on charged track momentum for the type-II events, we vary the nominal requirement from $p < 1.7$ GeV/ c to $p < 1.55$ GeV/ c , and the opening angle between two charged tracks from $\theta < 176^\circ$ to $\theta < 160^\circ$. The change in $N_{\psi(3686)}$ is taken as the corresponding systematic uncertainty.

D. LEB contamination

In the nominal measurement, the $E_{\text{visible}}/E_{\text{cm}} < 0.4$ requirement is used to suppress the LEB background events for the type-I and type-II events. The systematic uncertainty due to this requirement is assigned with alternative requirements of $E_{\text{visible}}/E_{\text{cm}} < 0.35$ and $E_{\text{visible}}/E_{\text{cm}} < 0.45$. The larger change in $N_{\psi(3686)}$ is assigned as the systematic uncertainty.

E. Extraction method of N^{obs}

The nominal measurement is performed by counting the events in the V_Z distributions in Fig. 4. To examine the systematic uncertainty associated with the counting method, we use an alternative method by fitting the V_Z distributions with three linearly added Gaussian functions to model the signal shape and a second order polynomial function to describe the non-collision background. The difference in the determined $N_{\psi(3686)}$ values between these two methods is taken as the systematic uncertainty.

F. Vertex requirement

To estimate the systematic uncertainties due to the vertex requirement, we examine the number of $\psi(3686)$ events after varying the nominal vertex requirements of

$V_r < 1$ cm to $V_r < 2$ cm, and from $|V_z| < 10$ cm to $|V_z| < 15$ cm. The change in the measured number of $\psi(3686)$ events is taken as the systematic uncertainty.

G. Scaling factor

The systematic uncertainty due to the scaling factor f is estimated with the alternatively measured luminosities with $e^+e^- \rightarrow \gamma\gamma$ events. The change of the re-measured $N_{\psi(3686)}$ is found to be negligible and this systematic uncertainty is therefore neglected.

H. π^0 mass requirement

A requirement of $|M_{\gamma\gamma} - M_{\pi^0}| < 0.015$ GeV/ c^2 has been imposed on the type-I events to suppress background. Its effect on the measured number of $\psi(3686)$ events is studied with an alternative requirement of $|M_{\gamma\gamma} - M_{\pi^0}| < 0.025$ GeV/ c^2 . The change in $N_{\psi(3686)}$ is taken as the systematic uncertainty.

I. Missing $N_{\text{good}} = 0$ hadronic events

We do not consider the $N_{\text{good}} = 0$ hadronic events in the nominal measurement. The topological analysis for the $\psi(3686)$ inclusive MC samples shows that most of these events come from well-known decay channels, such as $\psi(3686) \rightarrow X + J/\psi$ (where X denotes η , π^0 , $\pi^0\pi^0$, $\gamma\gamma$, etc.) and $\psi(3686) \rightarrow e^+e^-$, $\mu^+\mu^-$. The fraction of $N_{\text{good}} = 0$ hadronic events is $\sim 2.0\%$, and the pure neutral channels contribute about 1.0%.

We examine the effect of the $N_{\text{good}} = 0$ hadronic events as follows. A sample is selected using the requirements $N_{\text{good}} = 0$ and $N_\gamma > 3$, where the good charged tracks and showers are selected with the same criteria mentioned above. The $N_\gamma > 3$ requirement is used to sup-

press the $e^+e^- \rightarrow \gamma\gamma$ and beam-associated background events. Figure 6 shows the distributions of the total energy in the EMC, E_{EMC} , for the different data sets and inclusive MC samples. The events concentrated around the c.m. energy are mainly from the pure neutral hadronic candidates. The number of signal events is determined by a fit to the E_{EMC} distribution. In this fit, the signal is described by a Breit-Wigner function convolved with Crystal Ball function, the nonresonant background in the $\psi(3686)$ data sample is described by the shape of off-resonance data sample after luminosity normalization, and the other backgrounds are described by a polynomial function. For the 2021 data sample, the difference in the number of pure neutral hadronic events between the $\psi(3686)$ data and inclusive MC samples is 11%. Since the fraction of the pure neutral hadronic events is about 1% of the total selected hadronic events, the systematic uncertainty due to the missing $N_{\text{good}}=0$ hadronic events must be less than $11\% \times 1\% = 0.11\%$ for the 2021 data sample. With the same method, the systematic uncertainties for the 2009 and 2012 data samples are assigned as 0.38% and 0.31%, respectively.

J. Charged track multiplicity

To estimate the systematic uncertainty arising from the charged track multiplicity, we compare the directly calculated result as shown in Table 1 and that obtained with the unfolding method after including the $N_{\text{good}} \leq 1$ events. The differences in the numbers of $\psi(3686)$ events for the 2009, 2012 and 2021 data samples, which are 0.24%, 0.56%, and 0.26%, respectively, are taken as individual systematic uncertainties.

K. MC modeling

The systematic uncertainties due to MC modeling include the input branching fractions and the angular distri-

butions of the known and unknown decay modes in the $\psi(3686)$ inclusive MC sample. These uncertainties have been covered by those of the charged track multiplicity and the missing $N_{\text{good}}=0$ events. Hence no systematic uncertainty is assigned for the MC modeling.

L. Trigger efficiency

The trigger efficiencies for BESIII data were studied in 2010 [13] and 2021 [14]. The trigger efficiency for the $N_{\text{good}} \geq 2$ (type-II and type-III) events is found to be close to 100.0%, while it is 98.7% for the type-I events [13]. Since the fraction of the type-I events is only about 3% of the total selected hadronic events, the associated systematic uncertainty is negligible. The neutral channel trigger has been added since 2012, and the trigger efficiency for the type-I events is expected to be higher than before. Therefore, the systematic uncertainty associated with the trigger efficiency is negligible.

M. Branching fraction of $\psi(3686) \rightarrow \text{hadrons}$

The uncertainty of the branching fraction of $\psi(3686) \rightarrow \text{hadrons}$, 0.13% [1–3], is taken as a systematic uncertainty.

N. Total systematic uncertainty

The total systematic uncertainty for each $\psi(3686)$ data sample is obtained as the quadratic sum of all the systematic uncertainties.

VII. SUMMARY

By analyzing inclusive hadronic events, the number of $\psi(3686)$ events taken by the BESIII detector in 2021 is measured to be $(2259.3 \pm 11.1) \times 10^6$, where the uncertainty is systematic and the statistical uncertainty is negligible. The numbers of $\psi(3686)$ events taken in 2009 and

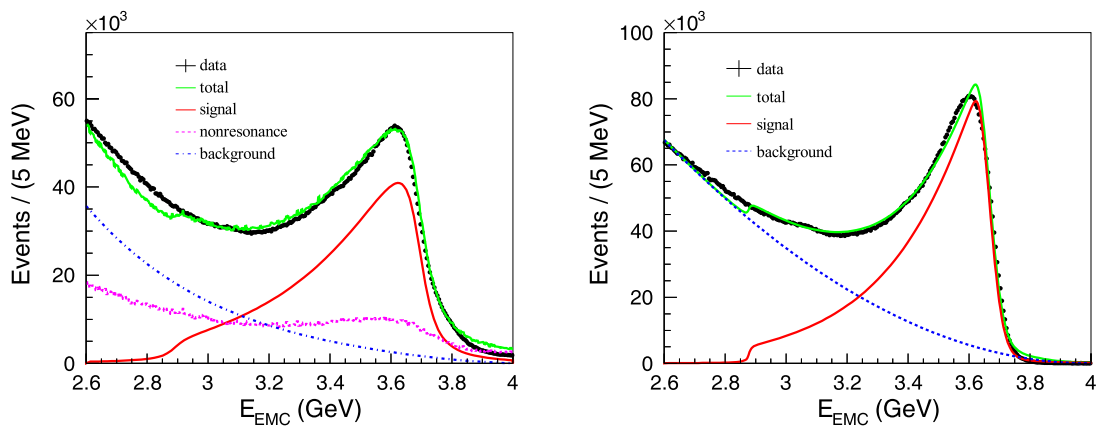


Fig. 6. (color online) Distributions of E_{EMC} for the $N_{\text{good}}=0$ hadronic events from the $\psi(3686)$ data (left) and inclusive MC (right) samples. The black points with error bar are data. The red lines are the signal shapes of neutral $\psi(3686)$ decays, the blue lines are the background shapes from $\psi(3686)$ decays, the pink line is the total background shape from nonresonant processes, and the green lines are the final fit curves.

2012 are also updated to be $(107.7\pm 0.6)\times 10^6$ and $(345.4\pm 2.6)\times 10^6$, respectively. Both are consistent with the previous measurements within one standard deviation, and a slight difference in the 2012 $\psi(3686)$ events relative to the previous one is caused by changing the off-resonance data from the previous τ -scan data to the off-resonance data at $\sqrt{s}=3.65$ GeV in 2021. The total number of $\psi(3686)$ events for the three data samples is obtained

to be $(2712.4\pm 14.3)\times 10^6$ by adding the above three yields linearly. This work provides an important parameter used in precision measurements of decays of the $\psi(3686)$ and its daughter charmonium particles.

ACKNOWLEDGEMENTS

The BESIII collaboration thanks the staff of BEPCII and the IHEP computing center for their strong support.

References

- [1] V. Luth, A. Boyarski, H. L. Lynch *et al*, *Phys. Rev. Lett.* **35**, 1124 (1975)
- [2] J. Z. Bai *et al.* (BES Collaboration), *Phys. Lett. B* **550**, 24 (2002)
- [3] R. L. Workman *et al.* (Particle Data Group), *PTEP* **2022**, 083C01 (2022)
- [4] M. Ablikim *et al.* (BESIII Collaboration), *Chin. Phys. C* **42**, 023001 (2018)
- [5] M. Ablikim *et al.* (BESIII Collaboration), *Nucl. Instrum. Meth. A* **614**, 345 (2010)
- [6] M. Y. Dong, Q. L. Xiu, L. H. Wu, *et al*, *Chin. Phys. C* **40**, 016001 (2016)
- [7] J. Allison, K. Amako, J. Apostolakis, *et al*, *IEEE Trans. Nucl. Sci.* **53**, 270 (2006)
- [8] S. Jadach, B. F. L. Ward and Z. Was, *Phys. Rev. D* **63**, 113009 (2001)
- [9] R. G. Ping, *Chin. Phys. C* **32**, 599 (2008)
- [10] J. C. Chen, G. S. Huang, X. R. Qi, *et al*, *Phys. Rev. D* **62**, 034003 (2000)
- [11] G. Balossini, C. M. Carloni Calame, G. Montagna, *et al*, *Nucl. Phys. B* **758**, 227 (2006)
- [12] M. Ablikim *et al.* (BESIII Collaboration), *Chin. Phys. C* **37**, 123001 (2013)
- [13] N. Berger, K. Zhu, Z. A. Liu, *et al*, *Chin. Phys. C* **34**, 1779 (2010)
- [14] M. Ablikim *et al.* (BESIII Collaboration), *Chin. Phys. C* **45**, 023002 (2021)